Journal of Physiology (1992), **451**, *pp.* 159–185
With 12 figures
Printed in Great Britain

KINETIC AND PHARMACOLOGICAL PROPERTIES OF THE M-CURRENT IN RODENT NEUROBLASTOMA × GLIOMA HYBRID CELLS

BY J. ROBBINS, J. TROUSLARD, S. J. MARSH AND D. A. BROWN

From the Department of Pharmacology, University College London, Gower Street, London WC1E 6BT

(*Received 6 June 1991*)

SUMMARY

1. The M-like current $I_{K(M,ng)}$ in differentiated NG108-15 mouse neuroblastoma × rat glioma hybrid cells has been studied using tight-seal, whole-cell patch-clamp recording.

2. When calculated from steady-state current–voltage curves, the conductance underlying $I_{K(M,ng)}$ showed a Boltzmann dependence on voltage with half-activation voltage $V_0 = -44$ mV (in 3 mM $[K^+]$) and slope factor (a) = 8·1 mV/e-fold increase in conductance. In 12 mM $[K^+]$ $V_0 = -38$ mV and $a = 6{\cdot}9$ mV. The deactivation reciprocal time constant accelerated with hyperpolarization with slope factor 17 mV/e-fold voltage change.

3. The reversal potential for deactivation tail currents varied with external $[K^+]$ as if P_{Na}/P_K were 0·005.

4. Steady-state current was increased on removing external Ca^{2+}. In the presence of external Ca^{2+}, reactivation of $I_{K(M,ng)}$ after a hyperpolarizing step was delayed. This delay was preceded by an inward Ca^{2+} current, and coincided with an increase in intracellular $[Ca^{2+}]$ as measured with Indo-1 fluorescence. Elevation of intracellular $[Ca^{2+}]$ with caffeine also reduced $I_{K(M,ng)}$.

5. $I_{K(M,ng)}$ was inhibited by external divalent cations in decreasing order of potency (mM IC_{50} in parentheses): Zn^{2+} (0·011) > Cu^{2+} (0·018) > Cd^{2+} (0·070) > Ni^{2+} (0·44) > Ba^{2+} (0·47) > Fe^{2+} (0·69) > Mn^{2+} (0·86) > Co^{2+} (0·92) > Ca^{2+} (5·6) > Mg^{2+} (16) > Sr^{2+} (33). This was not secondary to inhibition of I_{Ca} since: (i) inhibition persisted in Ca^{2+}-free solution; (ii) La^{3+} did not inhibit $I_{K(M,ng)}$ at concentrations which inhibited I_{Ca}; and (iii) organic Ca^{2+} channel blockers were ineffective. Inhibition comprised both depression of the maximum conductance and a positive shift of the activation curve. Addition of Ca^{2+} (10 μM free $[Ca^{2+}]$) or Ba^{2+} (1 mM total $[Ba^{2+}]$) to the pipette solution did not significantly change $I_{K(M,ng)}$.

6. $I_{K(M,ng)}$ was reduced by 9-amino-1,2,3,4-tetrahydroacridine (IC_{50} 8 μM) and quinine (30 μM) but was insensitive to tetraethylammonium (IC_{50} > 30 mM), 4-aminopyridine (> 10 mM), apamin (> 3 μM) or dendrotoxin (> 100 nM).

7. $I_{K(M,ng)}$ was inhibited by bradykinin (1–10 μM) or angiotensin II (1–10 μM), but not by the following other receptor agonists: acetylcholine (10 mM), muscarine (10 μM), noradrenaline (100 μM), adrenaline (100 μM), dopamine (100 μM), histamine

(100 μM), 5-hydroxytryptamine (10 μM), Met-enkephalin (1 μM), glycine (100 μM), γ-aminobutyric acid (100 μM) or baclofen (500 μM).

8. Inhibition of $I_{K(M,ng)}$ with Ba^{2+} did not change the zero-current potential but suppressed outward rectification of the current–voltage curve and facilitated repetitive action potential discharges produced by depolarizing current injections. This latter action was not imitated by tetraethylammonium, apamin or 4-aminopyridine.

9. It is concluded that $I_{K(M,ng)}$ resembles the M-current recorded in sympathetic ganglia in (i) kinetic behaviour, (ii) inhibition by transient rises in intracellular $[Ca^{2+}]$, and (iii) functional effects. It differs from the ganglionic M-current in certain pharmacological properties (sensitivity to divalent cations, organic K^+ channel blockers and receptor agonists).

INTRODUCTION

The M-current ($I_{K(M)}$) is a slow voltage-gated subthreshold potassium (K^+) current (see Brown, 1988, for review). It was originally identified in sympathetic neurones: in these cells it was inhibited by muscarine, hence the name (Brown & Adams, 1980; Constanti & Brown, 1981).

A comparable current has also been recorded from microelectrode-impaled cells of the NG108-15 clone of mouse neuroblastoma × rat glioma hybrid cells (Brown & Higashida, 1988*a*). However, in NG108-15 cells, the current was preferentially inhibited by the peptide bradykinin (Brown & Higashida, 1988*b*), and is relatively insensitive to activators of the native (m4) muscarinic receptor (Fukuda, Higashida, Kubo, Maeda, Akiba, Bujo, Mishina & Numa, 1988).

This raises the general question of how far the M-like current in NG108-15 cells might, or might not, be representative of M-currents in ganglion cells or other primary neurones. This is important because NG108-15 cells can be very convenient for studies on receptor–ion channel transduction mechanisms; for example, they can be readily used for DNA-transfection experiments (Fukuda *et al.* 1988; Neher, Marty, Fukuda, Kubo & Numa, 1988; Robbins, Caulfield, Higashida & Brown, 1991) or for GTP-binding protein antibody injections (McFadzean, Mullaney, Brown & Milligan, 1989), but the interpretation of such experiments clearly depends on how good a model this clonal cell line provides. This question of M-current definition is further highlighted by the observations of Beech & Barnes (1989) on salamander rod cells, in which they recorded a K^+ current with clear M-like kinetics but with noticeable pharmacological differences from the ganglionic M-current, and which they therefore designated I_{Kx} rather than $I_{K(M)}$.

Hence, in the present experiments, we have examined the M-like current in NG108-15 cells in more detail, using tight-seal, whole-cell patch recording. We have paid particular attention to four aspects of the current: its macroscopic kinetics, its sensitivity to Ca^{2+} and other divalent cations, its sensitivity to K^+ channel blocking agents, and its effect on cell excitability. For identification purposes, we refer to it throughout as $I_{K(M,ng)}$, to differentiate it from the ganglionic M-current, pending further definition. A brief abstract of some of our observations has been published (Brown & Robbins, 1990).

METHODS

NG108-15 mouse neuroblastoma × rat glioma cells were grown in 35 mm plastic dishes containing Eagle's minimal essential medium (EMEM) with 10% added fetal calf serum, and differentiated by adding 10 μM-prostaglandin E_1 with 50 μM-isomethylbutylxanthine as described by Docherty (1988). Between 4 and 9 days after differentiation, dishes were placed on the stage of an inverted microscope and the cells superfused at 5–10 ml min^{-1} and 35 °C with a bicarbonate-buffered salt solution containing (mM): NaCl, 120; KCl, 3; $NaHCO_3$, 22·6; $CaCl_2$, 2·5; $MgCl_2$, 1·2; HEPES, 5; D-glucose, 11. The pH was maintained at 7·36 by gassing continuously with 95% O_2/5% CO_2. A 'Ca^{2+}-free' solution was made by omitting $CaCl_2$, raising $MgCl_2$ to 5 mM and adding 100 μM-EGTA. Tetrodotoxin (TTX, 0·5 μM) was usually added to the superfusion fluid once recording was started.

Cells were patch clamped with electrodes filled with 90 mM-$KOOCCH_3$, 20 mM-KCl, 40 mM-HEPES, 3 mM-$MgCl_2$ and 3 mM-EGTA. (In some experiments, 1 mM-ATP and 1–2 mM-GTP were added, but this did not clearly affect the currents under study so were normally omitted.) Pipette resistances were 2–6 MΩ, and seal resistances > 10 GΩ. The reference electrode was a 3 M-KCl/agar bridge in contact with a separate pool of 3 M-KCl connected to ground via an Ag/AgCl pellet. To record Ca^{2+} currents, external NaCl was replaced with tetraethylammonium chloride (TEA, 120 mM) and $KOOCCH_3$ and KCl in the pipette solution replaced with 110 mM-CsCl. Pipette solution pH was adjusted to 7·39 with KOH or CsOH.

Membrane currents were recorded using discontinuous single-electrode voltage clamp (Axoclamp-2, Axon Instruments). Sample rate (4–7 kHz), capacitance neutralization, phase and gain were adjusted for optimum clamp fidelity as described by Finkel & Redman (1984). Currents were filtered at 0·3 kHz and recorded on-line using a pen-recorder (Gould 2400S). In addition, data filtered at 10 kHz were conveyed to a computer (Ness PC-286) via an analog-to-digital interface (Labmaster TL-1, Tecmar, Solon, USA) for further analysis using pClamp5 (Axon Instruments). The same software was used to generate stepped and ramped voltage commands. Voltage ramps were delivered at 2·5 mV s^{-1}, sufficiently slow for $I_{K(M,\,ng)}$ to be at steady state throughout (see Results).

Intracellular calcium measurements

Intracellular [Ca^{2+}] was estimated using Indo-1 fluorescence, by dual-wavelength emission, as described by Grynkiewicz, Poenie & Tsien (1985). For these experiments, cells were grown on polyornithine-coated glass coverslips, and the coverslips placed on the stage of an inverted microscope (Nikon 'Diaphot'). Cells were illuminated by a 75 W Xenon arc lamp (Osram XBO-75) via a quartz lens and 360 nm excitation filter (330–380 nm bandwidth). UV light was reflected by a 400 nm dichroic mirror and passed through an oil-immersion objective (Nikon × 40 fluorite, NA 1·3). To avoid photobleaching, neutral density filters reduced illumination by 0·6 log units and illumination was restricted to the cell recorded using a field diaphragm. Emitted light was collected from an aperture-limited field just greater than the area of the cell and split by a 430 nm dichroic mirror to two photomultipliers (Thorn EMI QL 30; power source PM 28B, 900 V DC) at 407 and 488 nm. Anodal currents were converted to voltage and fed into a differential amplifier providing continuous outputs of individual wavelength emissions and the ratio of emissions at 407 and 488 nm ($= R$). Voltage outputs were digitized via the TL-1 interface and data processed using pClamp.

Dye loading. Indo-1 was introduced into the cell by including it in the patch pipette solution (50–100 μM) or using the acetoxymethyl ester Indo-1/AM (Calbiochem). Cells were preloaded with 5 μM-Indo-1/AM for 45–60 min at 37 °C, then superfused with standard recording medium for 20–30 min to allow ester hydrolysis. For Indo-1 loading from the patch pipette, cells were equilibrated for at least 5 min after breakthrough: this sufficed to produce maximum, or near-maximum, fluorescence.

Calculation of intracellular [Ca^{2+}] and calibration. For each emission wavelength cell autofluorescence was measured under cell-attached configuration (before breakthrough) and amplifier outputs offset to zero. After breakthrough and loading, [Ca^{2+}] was estimated by the equation (Grynkiewicz *et al.* 1985):

$$[Ca^{2+}] = K_D\,(F_o/F_s)(R-R_{min})/(R_{max}-R),$$

where R = recorded 407/488 emission ration, R_{min} = minimal value of R at zero [Ca^{2+}], R_{max} =

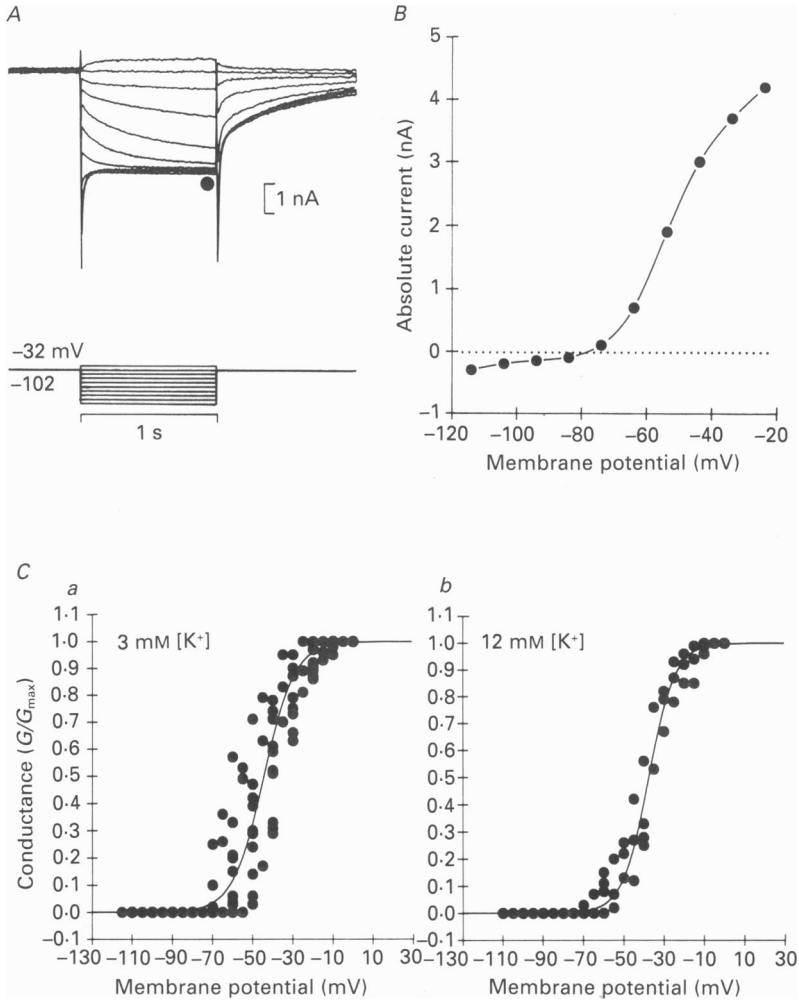

Fig. 1. Deactivation and activation of $I_{K(M,ng)}$. *A*, clamp currents (upper records) obtained during 1 s voltage steps (lower records) from a holding potential of −32 mV to command potentials (V_c) between −22 and −102 mV in 10 mV steps. Holding current +3·7 nA. Outward deactivating tail currents are observed during the hyperpolarizing steps, which reverse as V_c becomes negative to the reversal potential (V_r) for $I_{K(M,ng)}$. *B*, current level attained in *A* at the end of each 1 s voltage step (●, ordinate) plotted against command potential (abscissa). Currents are measured with respect to zero current recorded on detaching the pipette at the end of the experiment. *C*, steady-state activation curves for the conductance $G_{K(M,ng)}$ underlying $I_{K(M,ng)}$ obtained in thirteen experiments with 3 mM $[K^+]$ (*a*) and seven experiments with 12 mM $[K^+]$ (*b*). Cells were held at 0 mV, and subjected to a series of hyperpolarizing steps like those in *A* but 4 s long (to allow currents to reach a steady state). The amount of $I_{K(M,ng)}$ deactivated during each step was calculated from the amplitude of the deactivation current relaxations seen during the voltage step, and converted to change in conductance by dividing by the driving force $V_c - V_r$. Total conductance $G_{K(M,ng)}$ was calculated by cumulative addition (see Adams *et al.* 1982*a*) and expressed as a fraction of that attained at the holding potential (G_{max}). Points show data from individual experiments. Data from each experiment were processed individually and the best-fit Boltzmann relation $G/G_{max} = 1/\{1+\exp[(V_o - V_c)/a]\}$ (where $V_o = V_c$ when $G/G_{max} = 0{\cdot}5$) for that experiment determined

value of R at saturating [Ca^{2+}], and F_0/F_s = maximum excursion at 488 nm. Signals were calibrated in the cells (Popov, Gavrioly, Pozin & Gabbasov, 1988; Wahl, Lucherini & Gruenstein, 1990). Various concentrations of $CaCl_2$ were added to intracellular pipette solutions composed of 150 mM-KCl, 20 mM-HEPES and 10 mM-BAPTA, and the pH was adjusted to 7·2. The theoretical value of free [Ca^{2+}] was calculated using program 'React', version 2·01 (G. L. Smith, Chemistry Department, University College London). The solutions were then introduced into the cell under whole-cell patch-clamp configuration and the 407/488 nm emission ratio was measured. $(R-R_{min})/(R_{max}-R)$ values were plotted against calculated free [Ca^{2+}] and the constant $K_D(F_0/F_s)$ determined by linear regression. Under our optical conditions, R_{min} = 0·44, R_{max} = 4 and $K_D(F_0/F_s)$ = 1400 nM. Values for R_{max} were determined at the end of each run by permeabilizing the cell with a 200 mV hyperpolarizing pulse or by adding 10 μM-ionomycin.

Drugs and chemicals

The dichloride salts of Ca^{2+}, Cd^{2+}, Co^{2+}, Fe^{2+}, Mg^{2+}, Mn^{2+}, Ni^{2+} and Zn^{2+} were obtained from BDH. $GdCl_3$, $LuCl_3$ and $SmCl_3$ were obtained from Aldrich. $BaCl_2$, $CuCl_2$, $SrCl_2$, $LaCl_3$, tetrodotoxin (TTX), bradykinin, angiotension II, dopamine, noradrenaline, adrenaline, Met-enkephalin, acetylcholine, methacholine, *dl*-muscarine chloride, γ-aminobutyric acid, glycine, 9-amino-1,2,3,4-tetrahydroacridine (THA), tetraethylammonium chloride (TEA), 4-aminopyridine (4-AP), apamin, quinine and *d*-tubocurarine (dTC) were supplied by Sigma. Dendrotoxin was a gift from Professor J. O. Dolly (Biochemistry Department, Imperial College). Compounds were applied by superfusion in the concentrations indicated unless otherwise stated. Bradykinin was also applied by pressure ejection (3–55 kPa) from a micropipette placed in the superfusing medium upstream to the cell.

RESULTS

The observations described in this section are based on recordings from 233 NG108-15 cells differentiated with PGE_1 + IBMX (see Methods). All of these cells exhibited the M-like current $I_{K(M,ng)}$ as defined below. No such current was recorded from undifferentiated cells (i.e. cells grown in 10% fetal calf serum without added PGE_1 + IBMX).

Kinetics

To record $I_{K(M,ng)}$ we used the protocol previously employed in sympathetic neurones for detecting $I_{K(M)}$ (Adams, Brown & Constanti, 1982*a*): namely, the cell was clamped at a depolarized membrane potential (around −30 mV) and then stepped back to more hyperpolarized potentials for short periods. As shown in Fig. 1*A*, these steps induced slow inward current relaxations, which accelerated as the command potential became more negative, and reversed in direction at command potentials negative to about −90 mV. It was previously inferred that the comparable current relaxations in sympathetic ganglia were in fact outward tail currents resulting from the deactivation of a K^+ current, since the instantaneous current at the end of the step was smaller than that at the beginning, implying a fall in chord conductance (see Adams *et al.* 1982*a*). This is not obvious in Fig. 1*A* because repolarization has induced an additional fast inward current. This is a low-threshold Ca^{2+} current (Docherty, 1988), which is absent from sympathetic neurones. When the Ca^{2+} current was prevented by removing external Ca^{2+} ions, then a large fall in instantaneous current during the hyperpolarizing step was apparent (see Fig. 3*B*), just as in sympathetic neurones.

---

by least-squares regression analysis. The smooth curves show the composite Boltzmann relation for each of the two sets of experiments in low and high [K^+] respectively, reconstructed from arithmetic mean values for a and V_0.

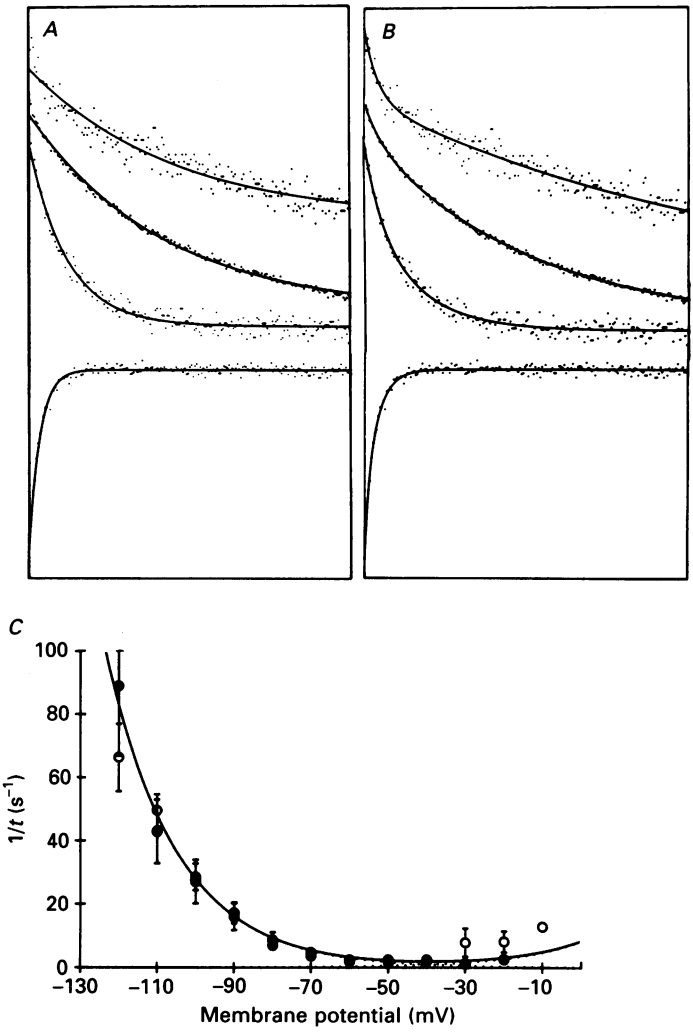

Fig. 2. Kinetics of $I_{K(M,ng)}$ deactivation. Records in *A* and *B* show deactivation tail currents recorded on stepping for 1 s to command potentials (V_c) of −40, −60, −80 and −100 mV from a holding potential (V_h) of −20 mV. Records were fitted with single (*A*) or double exponentials (*B*). Time constants in *A* are: −40 mV, 426 ms; −60 mV, 389 ms; −80 mV, 122 ms; and −100 mV, 31 ms. Corresponding time constants in *B* are: −40 mV, τ_1 39 ms, τ_2 1110 ms; −60 mV, τ_1 49 ms, τ_2 485 ms; −80 mV, τ_1 51 ms, τ_2 157 ms; −100 mV, τ_1 11 ms, τ_2 37 ms. *C* mean reciprocal time constant (τ^{-1}, s^{-1}) determined from best single-exponential fits to deactivation tails recorded in 3 mM [K^+] (○: $n = 5$) and 12 mM [K^+] (●; $n = 5$). Bars show S.E.M. The continuous curve is fitted to the equation $\tau^{-1} = \alpha + \beta$ where $\alpha = \alpha_0 \exp((V_c - V_0)/c)$ and $\beta = \beta_0 \exp((V_c - V_0)/c)$ and $\alpha_0 = 0{\cdot}2\ s^{-1}$, $\beta_0 = 3{\cdot}9\ s^{-1}$ and $c = 17{\cdot}2$ mV using data in 12 mM [K^+]. Dotted lines (where visible) show values for α and β separately.

The voltage range for $I_{K(M,ng)}$ activation was estimated by measuring the holding current level at the end of each hyperpolarizing and depolarizing step (Fig. 1*B*). The voltage-dependence of the underlying conductance change $G_{K(M,ng)}$ (Fig. 1*C*) was calculated by dividing the amplitude of each deactivation relaxation (dI (V)) by the

driving force, as given by the difference between the command potential (V) and the reversal potential for the relaxation (V_r) (see Adams *et al.* 1982*a*). To obtain the full activation range of $G_{K(M,ng)}$, cells were held at more positive potentials (~ 0 mV) and step hyperpolarized to -120 mV with 4 s steps (sufficiently long to ensure full decay of $I_{K(M,ng)}$). Such positive holding potentials were possible because the delayed rectifier current in these cells inactivates over several seconds (Robbins & Sim, 1990) and sustained Ca^{2+}-activated K^+ currents were suppressed by the high level of internal Ca^{2+} buffering (and possibly by the high internal Mg^{2+} concentrations; Cloues & Robbins, 1991), leaving $I_{K(M,ng)}$ as the only sustained outward current. In normal Krebs solution ($[K^+]_o = 3$ mM), activation of $G_{K(M,ng)}$ could be fitted with a Boltzmann equation with a half-maximal voltage (V_0) of $-44{\cdot}2 \pm 2{\cdot}2$ mV (mean ± S.E.M.) and slope factor (a) of $8{\cdot}1 \pm 0{\cdot}5$ mV/e-fold change in conductance (Fig. 1*Ca*; $n = 13$). In order to resolve the threshold, experiments were repeated in 12 mM $[K^+]_o$, so that relaxations were inverted negative to -60 mV. Under these conditions the activation curve was more positive (V_0 $-37{\cdot}5 \pm 1{\cdot}4$ mV) and rather steeper ($a = 6{\cdot}9 \pm 0{\cdot}6$ mV) (Fig. 1*Cb*; $n = 7$). In seven paired comparisons on single cells studied sequentially in 3 and 12 mM $[K^+]$, the mean shift of V_0 was $10{\cdot}4 \pm 3{\cdot}3$ mV.

Time constants

As indicated in Fig. 1*A*, the deactivation relaxations accelerated with increasing hyperpolarization. While this current decay frequently followed a single-exponential time course, a better fit could usually be obtained using two exponentials, particularly at more positive command potentials (Fig. 2). However, the faster time constant component was of variable magnitude, and did not change in any consistent way with command voltage. For these reasons, the voltage dependence of the relaxations was assessed using best-fit single exponentials. The voltage dependence of the reciprocal time constant (τ^{-1}) could be fitted with a Boltzmann equation with a slope factor of about 17 mV at command potentials negative to -60 mV (Fig. 2*C*), i.e. about half of that for the steady-state conductance in high $[K^+]$. This can be interpreted by assuming a simple closed–open scheme for the individual channels, with a similar voltage dependence of the opening and closing rate constants (at least over the voltage range examined) and that the time constant for the current deactivation is determined almost exclusively by the closing rate constant (see Adams *et al.* 1982*a*). The conformational change might then be governed by a single voltage-sensing particle of effective valency about $+3$.

As recently pointed out by Kelly & Pennefather (1989) and Gruner, Marrion & Adams (1989), the original scheme of Adams *et al.* (1982*a*) is almost certainly an oversimplification. In particular (and as noted by Kelly & Pennefather, 1989), the time constant does not accelerate with depolarization in the manner predicted by Adams *et al.* (1982*a*), suggesting a much slower opening rate constant (see Fig. 2*C*). However, present data do not warrant any more elaborate treatment, and so the original scheme of Adams *et al.* (1982*a*) is adhered to for comparability (see Discussion).

Potassium (K^+) dependence

The reversal potential for the current deactivation relaxations (V_r) varied with external $[K^+]$ between 0·5 and 24 mM according to a constant-field equation assuming a permeability ratio P_{Na}/P_K of 0·005. Between 9 and 24 mM, the relationship was linear, with slope 61 mV/e-fold change in $[K^+]_o$. An alternative explanation for

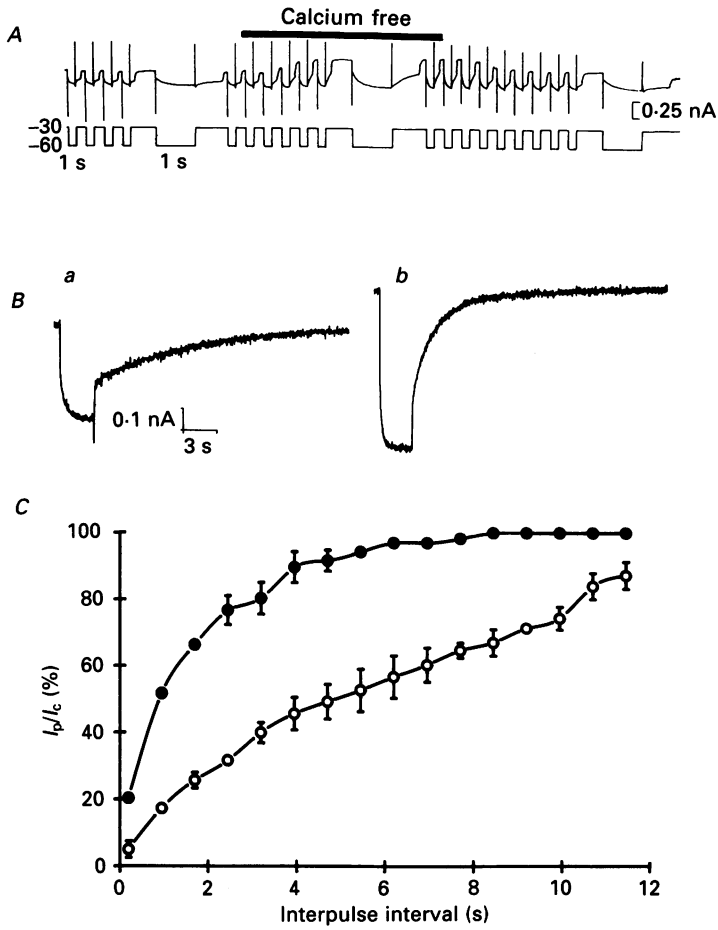

Fig. 3. Effect of removing external Ca^{2+} on $I_{K(M,ng)}$. *A* shows a continuous trace of membrane current (upper record) and voltage (lower record) recorded first in normal (2·5 mM $[Ca^{2+}]$, 1·2 mM $[Mg^{2+}]$) Krebs solution and then on briefly replacing this with a solution containing 0 mM-added Ca^{2+}, 5 mM-Mg^{2+} and 100 μM-EGTA ('Calcium free', at bar). The membrane potential was held at −30 mV and commanded to −60 mV for 1 s every 60 s to deactivate $I_{K(M,ng)}$. Deactivation is signalled by a slow inward current relaxation (see Fig. 1*A*). (The recorder was accelerated ×100 or ×500 for the duration of each hyperpolarizing command.) Note that both the outward holding current and the amplitude of the slow deactivation relaxations increased during superfusion with the Ca^{2+}-free solution. *B*, expanded records showing deactivation and reactivation of $I_{K(M,ng)}$ during and after longer (3 s) 30 mV hyperpolarizing steps in 2·5 mM $[Ca^{2+}]$ (*Ba*), and 0 mM $[Ca^{2+}]$ (*Bb*). Note that the fast inward current accompanying the repolarizing step in 2·5 mM $[Ca^{2+}]$ is absent in 0 mM $[Ca^{2+}]$. *C*, 'envelope of tails' test for $I_{K(M,ng)}$ reactivation after a hyperpolarizing step. Two 3 s hyperpolarizing steps from −30 to −60 mV were delivered at variable interpulse intervals, and the amplitude of the deactivation relaxation induced by the second voltage step (I_p) was used to calculate the magnitude of $I_{K(M,ng)}$ at different times after the first voltage step. This was expressed as a percentage of corresponding deactivation relaxation observed during the first voltage step (I_c). The graphs show the ratio I_p/I_c (×100%) plotted against interpulse interval(s) for three cells in 2·5 mM $[Ca^{2+}]$ (○) and three cells in 0 mM $[Ca^{2+}]$ (●). Bars are S.E.M. Time constants for reactivation were about 9 s in 2·5 mM $[Ca^{2+}]$ and 2 s in 0 mM $[Ca^{2+}]$.

the deviation from a K^+ diffusion potential below 9 mM might therefore be that the $[K^+]$ in the recirculating 50 ml of bathing solution was raised slightly above the nominal value by leakage from the 3 M-KCl bridge electrode (see Robbins & Sim, 1990). In either case, the reversal potential changes accorded with a predominantly K^+ current.

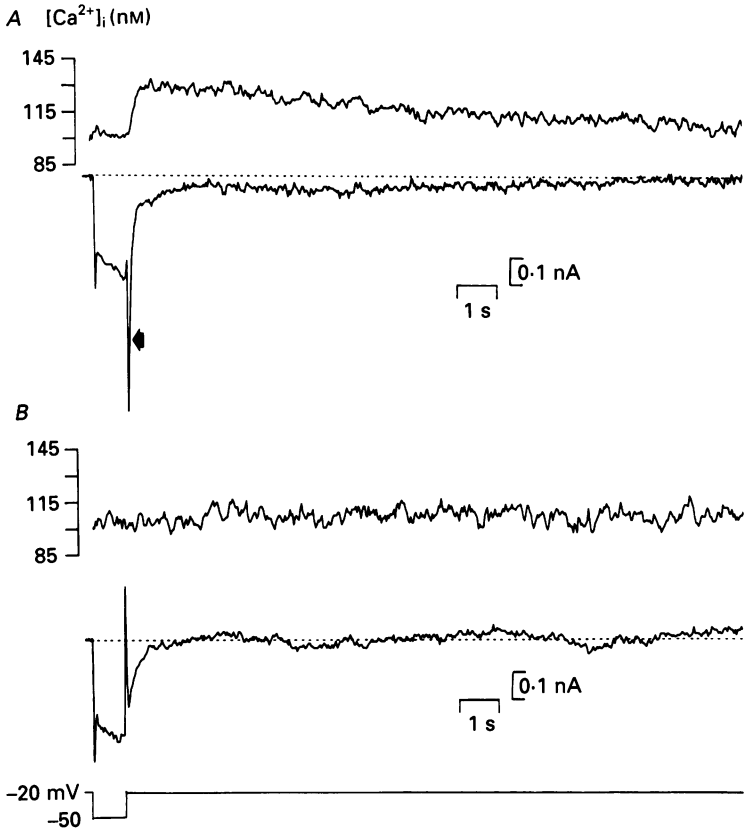

Fig. 4. Simultaneous measurements of intracellular $[Ca^{2+}]$ by Indo-1 fluorescence (upper traces; see Methods for details) and membrane current (lower trace) during and after a 1 s hyperpolarizing step from −20 to −50 mV. The records in *A* and *B* are from two different cells. Patch electrodes contained 100 μM-Indo-1 with 0·1 mM-added BAPTA. In cell *A* repolarization is accompanied by a transient inward current (arrowed) and a rise in internal $[Ca^{2+}]$, with a corresponding delay in the full reactivation of $I_{K(M,ng)}$ (as in Fig. 3). In cell *B* the transient inward current is absent: there is no significant rise in internal $[Ca^{2+}]$ and $I_{K(M,ng)}$ now reactivates rapidly.

Pharmacology

Calcium ions

In some (Tokimasa & Akasu, 1990) but not all (Adams, Brown & Constanti, 1982*b*; Marrion, Smart, Marsh & Brown, 1989*b*) previous tests on sympathetic ganglia, $I_{K(M)}$ decreased on removing extracellular Ca^{2+}. In NG108-15 cells, removal of external Ca^{2+} (with elevation of $[Mg^{2+}]_o$ to 5 mM) had two effects on $I_{K(M,ng)}$ (Fig. 3). First, it *increased* the amount of $I_{K(M,ng)}$ recorded at the depolarized holding potential, by

51 ± 8·8 % (n = 14). Second, it appeared to *accelerate* the reactivation of the current when the cell was repolarized after a hyperpolarizing step (Fig. 3*B*). In contrast, there was no significant change in the rate of deactivation during the hyperpolarizing step itself over the range −10 to −110 mV (n = 6).

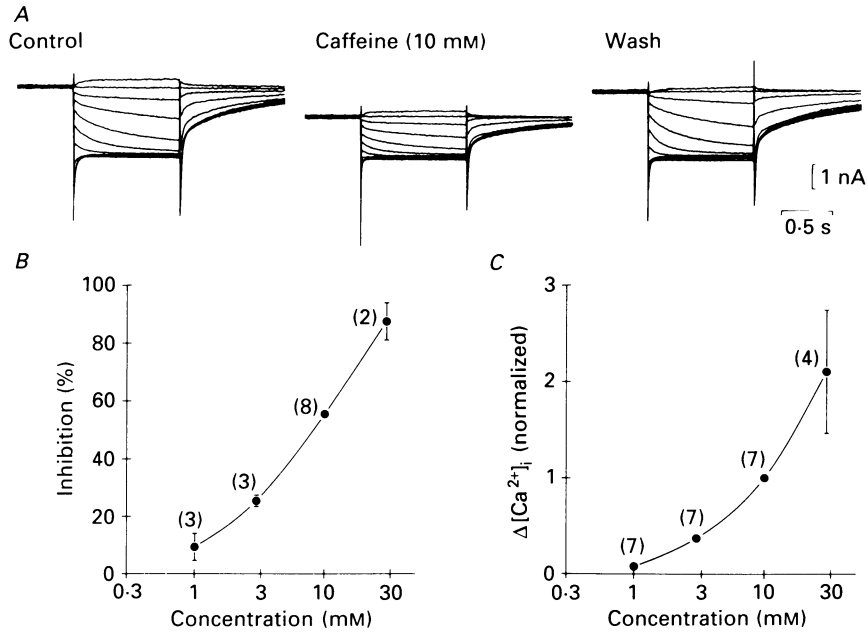

Fig. 5. Effects of external caffeine on $I_{K(M,ng)}$ (*A* and *B*) and on intracellular [Ca^{2+}] (*C*). *A*, families of membrane currents induced by 1 s voltage steps from a holding potential of −30 mV to command potentials of −20 to −110 mV in 10 mV steps (see Fig. 1*A*), recorded before ('Control'), during and 3 min after exposure to 10 mM-caffeine in the superfusion fluid. Note that caffeine reduces the outward holding current and reduces the amplitude of the $I_{K(M,ng)}$ deactivation tail currents during the hyperpolarizing steps. *B*, relationship between percentage inhibition of the $I_{K(M,ng)}$ deactivation tail current (measured at a command potential of −60 mV: ordinate) and the concentration of caffeine (abscissa). Each point is the mean of the number of experiments shown in parentheses; bars are S.E.M. *C*, relation between calculated increase in intracellular [Ca^{2+}] (measured in Indo-1/AM-loaded cells (see Methods) and expressed as a fraction of the increase in the same cell produced by 10 mM-caffeine) and the concentration of caffeine. Each point represents the mean of several measurements on different cells (number of cells in parentheses); bars are S.E.M.

The slow redevelopment of the outward current in normal (Ca^{2+}-containing) solution might be due to the activation of a countervailing inward current by the depolarization, rather than to a slow reactivation of $I_{K(M,ng)}$ *per se*. To test this, reactivation of $I_{K(M,ng)}$ was assessed from the amplitude of the deactivation relaxations induced by a second hyperpolarizing step applied at variable times after the first step. The time constant for reactivation in normal solution was about 9 s and was reduced to about 2 s on removing external Ca^{2+} (Fig. 3*C*). This 'envelope test' thus confirms that external Ca^{2+} slows $I_{K(M,ng)}$ reactivation itself.

As noted in Fig. 1, in these cells repolarization usually activated a low-threshold

Ca^{2+} current. Since this current was prevented by removing external Ca^{2+} (see Fig. 3), one interpretation of these experiments is that the entry of Ca^{2+} transiently depressed $I_{K(M,ng)}$. To test this further we recorded changes in intracellular [Ca^{2+}] produced by comparable voltage steps in cells filled with the Ca^{2+} indicator Indo-1 (Fig. 4). No change in resting signal could be detected during the 1 s hyperpolarizing step itself. However, cells exhibiting a transient inward current at the onset of the repolarizing step showed a clear increase in the Indo-1 signal, and a corresponding slow component of $I_{K(M,ng)}$ reactivation (Fig. 4*A*). In contrast, cells which did not exhibit an inward transient current on repolarizing showed no Indo-1 signal and a faster outward current reactivation (Fig. 4*B*). Rises in total intracellular [Ca^{2+}] measured with Indo-1 were readily apparent when the pipette was filled with 0·1 mM-Indo-1, either alone or with a low concentration of added buffer (0·1–0·3 mM-BAPTA or EGTA), but no clear change in Indo-1 signal was seen when the pipette contained 0·1 mM-Indo-1 plus 1–3 mM-EGTA or BAPTA. We assume that high buffering with Indo-1 or EGTA blunted the [Ca^{2+}] rise in the interior of the cell while still allowing submembrane [Ca^{2+}] to rise to a level capable of reducing $I_{K(M,ng)}$, in the manner predicted for increased intracellular buffering by Sala & Hernandez-Cruz (1990).

In sympathetic neurones $I_{K(M)}$ can be depressed when intracellular [Ca^{2+}] is raised by other means, such as the application of caffeine (Pfaffinger, Leibowitz, Subers, Nathanson, Almers & Hille, 1988; Akaike & Sadoshima, 1989; Marrion, Marsh, Burbach, Brown & Adams, 1989) or flash photolysis of Nitr-5 (Marrion, Zucker, Marsh & Adams, 1991). We therefore tested the effect of caffeine on intracellular [Ca^{2+}] and on $I_{K(M,ng)}$ in NG108-15 cells. In Indo-1/AM-loaded (unclamped) cells, caffeine produced a progressive increase in intracellular [Ca^{2+}] over the concentration range 1–30 mM (Fig. 5*C*), ranging (at 10 mM) from 46 nM to about 2 μM. In a further eight cells we confirmed that 10 mM-caffeine increased intracellular [Ca^{2+}] by 525 ± 95 nM under whole-cell voltage-clamp conditions with 0·1 mM-Indo-1 added to the pipette solution (already containing 3 mM-EGTA). Caffeine produced a progressive inhibition of $I_{K(M,ng)}$ over the same concentration range (1–30 mM) as that which raised intracellular [Ca^{2+}] (Fig. 5*A* and *B*). Caffeine also produced baseline current oscillations (at a mean frequency of $0{\cdot}024 \pm 0{\cdot}001$ Hz, $n = 6$) which persisted for up to 30 min after washing out the caffeine. These resembled those previously observed in frog sympathetic neurones by Kuba (1980).

In contrast (though also in agreement with Pfaffinger *et al.* 1988), varying the steady resting level of [Ca^{2+}] in the pipette solution between calculated values ranging from < 1 nM to 10 μM (by varying the concentrations of EGTA and added $CaCl_2$) did not produce any obvious change in the amplitude or kinetics of $I_{K(M,ng)}$ recorded in different cells following breakthrough. We tested this more carefully by first patching with an electrode containing < 1 nM calculated free [Ca^{2+}], then removing the patch pipette and re-patching with another electrode containing > 5 μM calculated free [Ca^{2+}]. Although the leak/seal conductance change (in a non-systematic manner) neither the steady-state amplitude of $I_{K(M,ng)}$ nor the time and voltage dependence of the deactivation showed any substantial change ($n = 3$).

Blocking action of external divalent cations

The increased amplitude of $I_{K(M,ng)}$ seen on reducing external [Ca^{2+}] (Fig. 3) implies that $I_{K(M,ng)}$ might be further inhibited by raising external Ca^{2+}. To test this, $[Ca^{2+}]_o$ was varied between 0·5 and 30 mM in the presence of 5 mM [Mg^{2+}]. A progressive inward current occurred, and the $I_{K(M,ng)}$ deactivation relaxations

TABLE 1. Concentrations of metal cations which produced 50% inhibition (IC_{50}) of: $I_{K(M,ng)}$; peak Ca^{2+} current ($I_{Ca(p)}$); and Ca^{2+} current recorded at the end of a 500 ms depolarization ($I_{Ca(s)}$)

Ion	$I_{K(M,ng)}$	$I_{Ca(p)}$	$I_{Ca(s)}$
Zn^{2+}	0·011 (0·010/0·012)	0·105 (0·099/0·110)	0·238 (0·223/0·254)
Cu^{2+}	0·018 (0·015/0·021)	0·040 (0·037/0·043)	0·055 (0·051/0·060)
Cd^{2+}	0·070 (0·064/0·076)	0·028 (0·025/0·032)	0·025 (0·022/0·030)
Ni^{2+}	0·438 (0·395/0·485)	0·070 (0·061/0·080)	0·367 (0·322/0·417)
Ba^{2+}	0·469 (0·412/0·535)	C	C
Fe^{2+}	0·687 (0·635/0·743)	1·30 (1·04/1·64)	1·53 (1·20/1·95)
Mn^{2+}	0·863 (0·754/0·987)	0·697 (0·645/0·753)	0·635 (0·580/0·696)
Co^{2+}	0·920 (0·886/0·955)	0·826 (0·773/0·883)	1·10 (0·97/1·23)
Ca^{2+}	5·63 (5·16/6·14)	C	C
Mg^{2+}	16·3 (16·1/16·7)	6·82 (6·22/7·48)	10·7 (10·6/10·8)
Sr^{2+}	32·9 (28·2/38·4)	C	C
Sm^{3+}	0·0010 (0·0009/0·0011)	0·068 (0·051/0·091)	0·012 (0·0101/0·015)
Gd^{3+}	0·0037 (0·0031/0·0043)	0·017 (0·014/0·019)	0·0040 (0·0038/0·0047)
Lu^{3+}	0·084 (0·076/0·091)	0·057 (0·051/0·063)	0·014 (0·014)
La^{3+}	2·13 (1·80/2·52)	0·077 (0·061/0·098)	0·017 (0·013/0·023)

Inhibition of $I_{K(M,ng)}$ was measured from the amplitude of the deactivation tail current during a 1 s step from −30 to −60 mV. Inhibition of I_{Ca} was measured from the amplitudes of the net inward current evoked by 500 ms depolarizing steps from −90 mV to near-zero potential, using the recording solutions described in Methods. (See Fig. 6 for sample records.) For each ion, data from four to six experiments were pooled and best fits to the function $y = [M]/([M]+IC_{50}) \times 100\%$ (where y = % percentage inhibition of recorded current and [M] = concentration of metal cation, mM) were determined by a non-linear iterative curve-fitting procedure. Numbers give calculated mean IC_{50} (mM); numbers in parentheses give 95% confidence limits. C = charge carrier.

produced by a 30 mV hyperpolarizing step from −30 mV holding potential were reduced, with an effective IC_{50} of about 5 mM. This was not due to a shift in reversal potential, which remained essentially unchanged.

Similar tests were completed for a range of other divalent cations (in the presence of 1·2 mM [Mg^{2+}] and 2·5 mM [Ca^{2+}]). These are summarized in Table 1. It is clear that the inhibitory action of Ca^{2+} was shared by all of the divalent cations tested, in decreasing order of potency: $Zn^{2+} > Cu^{2+} > Cd^{2+} > Ni^{2+} > Ba^{2+} > Fe^{2+} > Mn^{2+} > Co^{2+} > Ca^{2+} > Mg^{2+} > Sr^{2+}$. In each case block was unaccompanied by any significant shift in reversal potential.

Since many of these ions are also capable of blocking Ca^{2+} currents (e.g. Hagiwara & Byerly, 1981), we compared their effect on the Ca^{2+} current evoked by step depolarizations from −90 mV to near-zero mV recorded using 2·5 mM [Ca^{2+}] as charge carrier (Docherty, 1988; see Methods) (Fig. 6). Excluding Ba^{2+}, Ca^{2+} and Sr^{2+} (which act as charge carriers for I_{Ca}), there was a clear correspondence between the concentration required to block I_{Ca} and that which blocked $I_{K(M,ng)}$ for most of the

ions tested (Fig. 7). The principal exceptions were Zn^{2+} (Fig. 6) and Fe^{2+}, which were about 21 and 2·2 times more effective respectively against $I_{K(M,ng)}$ than against I_{Ca}.

This raises the question whether the ability of some of these divalent cations to inhibit $I_{K(M,ng)}$ might, in fact have been secondary to I_{Ca} inhibition. (This would then

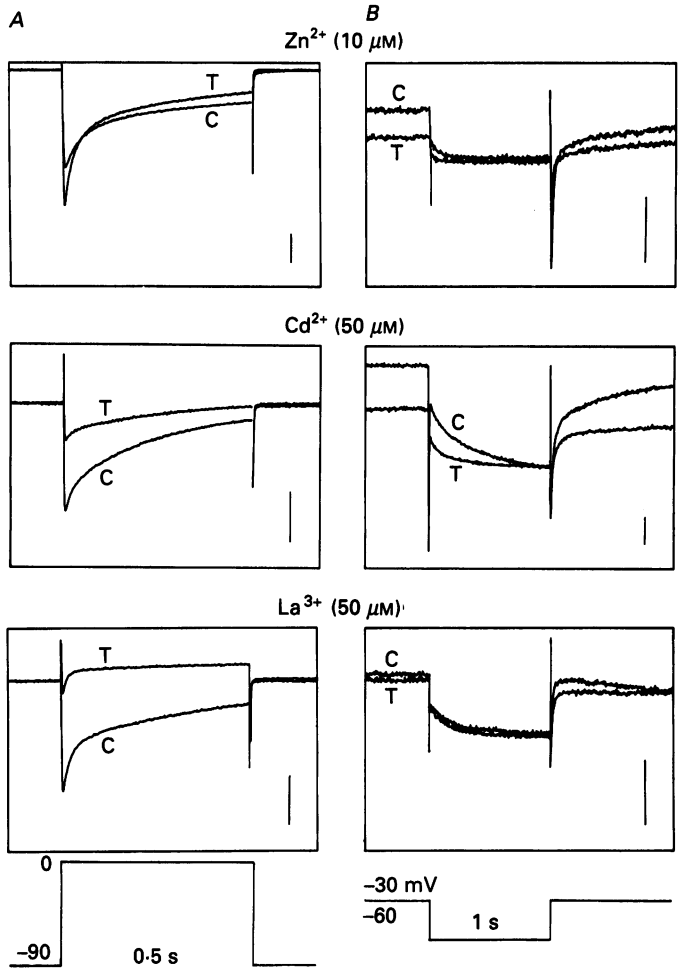

Fig. 6. Effects of 10 μM-Zn^{2+}, 50 μM-Cd^{2+} and 50 μM-La^{3+} on Ca^{2+} currents (*A*) and $I_{K(M,ng)}$ (*B*). Ca^{2+} currents were recorded using Cs^+-filled pipettes (see Methods), and were activated by applying 0·5 s, +90 mV steps from a holding potential of −90 mV. $I_{K(M,ng)}$ was recorded with K^+-filled pipettes (from different cells), and was pre-activated by depolarizing to −30 mV: records show deactivation of $I_{K(M,ng)}$ on stepping for 1 s to −60 mV. Each pair of records shows currents observed before (C) and after (T) adding the metal cation to the superfusion fluid (as Cl^- salt). Note that Zn^{2+} reduced $I_{K(M,ng)}$ more than I_{Ca}, whereas La^{3+} reduced I_{Ca} more than $I_{K(M,ng)}$. Calibrations: *A*, 1 nA; *B*, 0·5 nA.

imply that $I_{K(M,ng)}$ was really a species of Ca^{2+}-activated K^+ current, as earlier suggested for $I_{K(M)}$ in sympathetic neurones; Koketsu, Akasu & Miyagawa, 1982). We tested this in three ways.

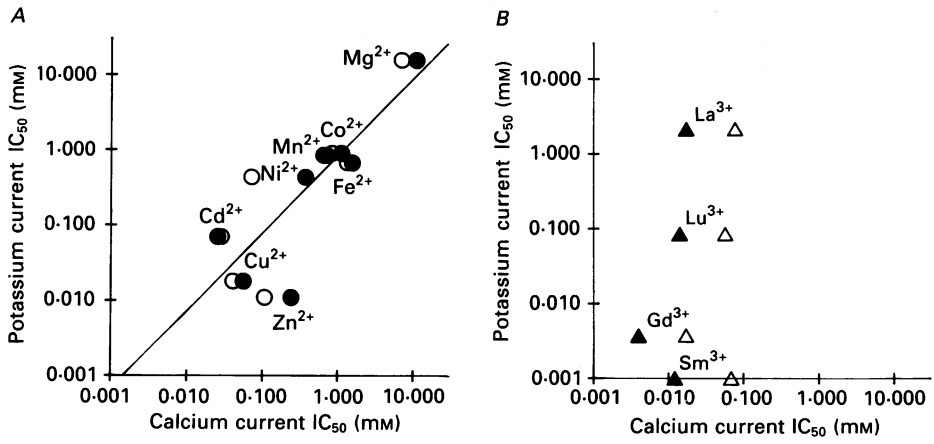

Fig. 7. Relation between the concentrations of divalent (*A*) and trivalent (*B*) metal cations required to inhibit $I_{K(M,ng)}$ (ordinates) and I_{Ca} (abscissae) by 50 % (IC_{50}). Inhibition of $I_{K(M,ng)}$ was measured from the amplitude of the deactivation relaxations observed on hyperpolarizing cells from −30 to −60 mV. Inhibition of I_{Ca} was measured from the amplitudes of the inward currents observed on stepping for 500 ms from −90 to 0 mV (cf. Fig. 6). Each point is the mean of at least three experiments; actual values are given in Table 1. Open symbols refer to measurements of peak I_{Ca}, filled symbols to I_{Ca} at the end of the 500 ms step. The line in *A* is the line of least-squares regression (correlation coefficient = 0·98; $P < 0·005$).

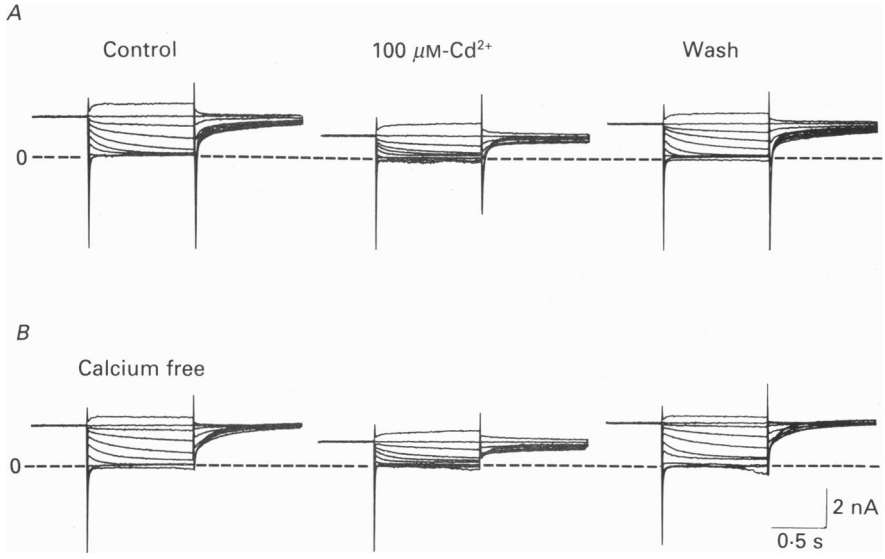

Fig. 8. Inhibition of $I_{K(M,ng)}$ by 100 μM-Cd^{2+} recorded in normal Krebs solution containing 2·5 mM [Ca^{2+}] and 1·2 mM [Mg^{2+}] (*A*) and then after replacing this solution with one containing 0 mM [Ca^{2+}], 5 mM [Mg^{2+}] and 0·1 mM EGTA (B, 'Calcium-free'). Records show families of currents evoked by 1 s voltage steps from a holding potential of −30 mV to command potentials between −20 and −100 mV in −10 mV steps (see Fig. 1*A*). Note that, in calcium-free solution, the transient inward Ca^{2+} current at the end of the hyperpolarizing command steps is lost, but that Cd^{2+} still inhibits $I_{K(M,ng)}$.

(i) First, we assessed the effect of one such Ca^{2+} channel blocking ion (Cd^{2+}) in the presence and absence of external Ca^{2+}. As shown in Fig. 8, Cd^{2+} reduced $I_{K(M,ng)}$ to the same extent under both conditions. The IC_{50} value in Ca^{2+}-free solution was $81 \pm 9{\cdot}3$ μM ($n = 5$), i.e. similar to that in the presence of Ca^{2+} (cf. Table 1). Other

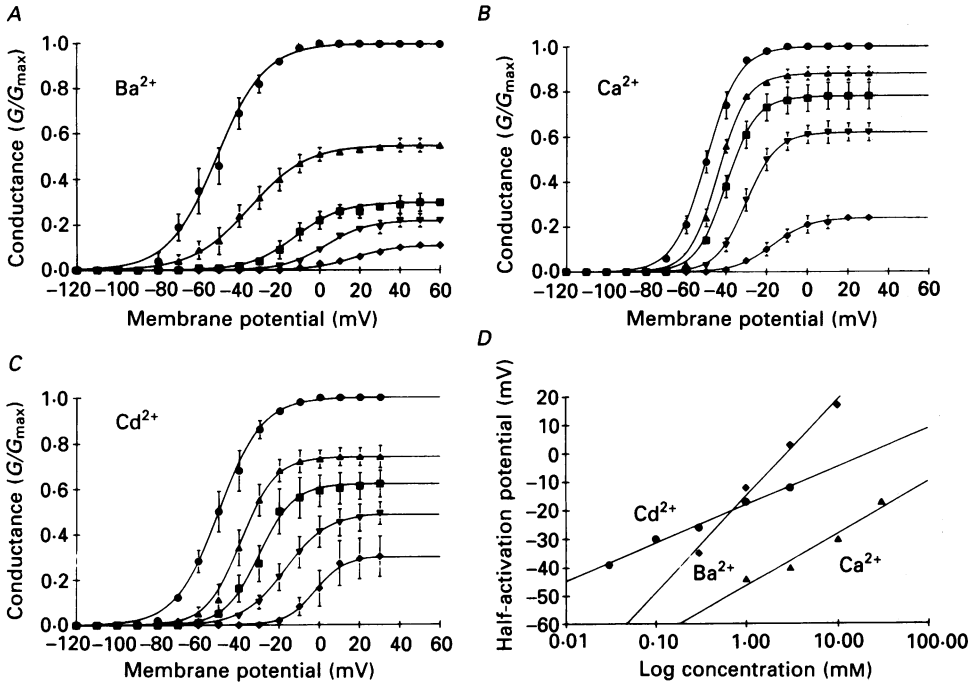

Fig. 9. Effects of external Ba^{2+} (*A*), Ca^{2+} (*B*) and Cd^{2+} (*C*) on activation curves for the conductance underlying $I_{K(M,ng)}$. Graphs show normalized conductance (G/G_{max}) plotted against command voltage recorded in the presence of increasing concentrations of the divalent cations, and determined as described in Fig. 1*C*. Ba^{2+} and Cd^{2+} were added in the presence of 2·5 mM [Ca^{2+}] and 1·2 mM [Mg^{2+}]; Ca^{2+} was added in the presence of 5 mM [Mg^{2+}]. Each point is the mean of five cells (*A* and *C*) or three cells (*B*). Curves are best-fit Boltzmann functions (see Fig. 1*C*). Symbols: *A*: ●, 0; ▲, 0·3; ■, 1; ▼, 3; and ◆, 10 mM [Ba^{2+}]; *B*: ●, 0; ▲, 1; ■, 3; ▼, 10 mM and ◆, 30 mM [Ca^{2+}]; *C*: ●, 0; ▲, 0·03; ■, 0·1; ▼, 1; and ◆, 3 mM [Cd^{2+}]. *D*, plot of half-activation voltage (V_0) for the residual (unblocked) conductance (ordinate) against divalent cation concentration (abscissa, logarithmic scale). Lines are least-square regressions for the relation $V_0' = V_0 \exp([M^{2+}]/x)$ where V_0' = half-activation voltage recorded in the presence of divalent cations, V_0 = corresponding voltage in the absence of the divalent cations and x is a constant. Values for x (mV) were: Ba^{2+}, 14·7 (◆); Ca^{2+}, 8·0 (●); Cd^{2+}, 5·8 (▲).

divalent cations (Co^{2+}, Mn^{2+}, Ni^{2+} and Ba^{2+}) also inhibited $I_{K(M,ng)}$ in Ca^{2+}-free solution.

(ii) We also tested four *trivalent* cations, i.e. Sm^{3+}, Gd^{3+}, Lu^{3+} and La^{3+}. Here there was a clear discrepancy between the concentrations required to block the two currents (Figs 6 and 7). For example, La^{3+} blocked I_{Ca} at 100-fold lower concentrations than those required to block $I_{K(M,ng)}$ (Fig. 9) whereas Sm^{3+} was 12 times more effective against $I_{K(M,ng)}$ than against I_{Ca} (Table 1).

(iii) Neither nifedipine ($n = 2$) nor ω-conotoxin ($n = 2$) reduced $I_{K(M,ng)}$ when applied in concentrations (5 and 0·1 μM respectively) which blocked the high-threshold components of I_{Ca} in these cells (Docherty, 1988; M. P. Caulfield, J. Robbins & D. A. Brown, unpublished).

Voltage-dependence of divalent cation block. Beech & Barnes (1989) reported that block of the M-like current I_{Kx} by Ba^{2+} in salamander rods was accompanied by a

TABLE 2. Calculated binding constants for divalent cation inhibition of $I_{K(M,ng)}$ (see eqn (1))

Cation	K_B (mM)	$K_{B(V_0)}$ (mM)	$\frac{K_B}{K_{B(V_0)}}$	Slope factor b (mV)	Hydrated ionic radius* (nm)
Cd^{2+}	1·8	0·2	9	5·8	0·425
Ca^{2+}	16·3	6·7	2·4	8·0	0·407
Ba^{2+}	1·0	0·2	5	14·7	0·399

* From Shannon (1976).

large positive shift in its activation curve. We therefore tested the effect of three divalent cation blockers – Ca^{2+}, Ba^{2+} and Cd^{2+} – on the voltage activation of $G_{K(M,ng)}$ (Fig. 9). In these experiments, the cells were again held at a positive potential (+30 or +60 mV) and conductance–voltage curves determined from the amplitudes of the deactivation relaxations (cf. Fig. 1*C*) in the presence of increasing concentrations of divalent cation. All three cations produced both a depression of the peak conductance and a rightward shift of the activation curve. The shift of the half-activation voltage (V_0) showed an approximately exponential dependence on cation concentration (Fig. 9*D*), but with varying slopes. Slope factors per e-fold change in cation concentration were 5·8 mV for Cd^{2+}, 8·0 mV for Ca^{2+} and 14·7 mV for Ba^{2+}.

These varying slopes suggest that a simple surface charge-screening or surface binding mechanism in unable to fully explain the shift (cf. McLaughlin, Szabo & Eisenman, 1971; Ohmori & Yoshii, 1975). Instead, we found that the experimental data could better be fitted by assuming a combination of voltage-dependent channel block and voltage-independent channel closure. Thus, if one assumes two binding sites, one with dissociation constant K_B outside the membrane field and insensitive to voltage, and one within the membrane field sensitive to voltage, with dissociation constant $K_{B(V)}$, and that occupation of either site closes the channel, then the proportion of open channels at voltage V might be given by (cf. Woodhull, 1973):

$$P_o(V) = \left(1 + \exp\frac{V_0 - V}{a} + \frac{[B]}{K_B} + \frac{[B]}{K_{B(V)}}\right)^{-1} \quad (1)$$

where: [B] = concentration of blocking ion (mol l^{-1}), $K_{B(V)} = K_{B(V_0)} \exp V_0 - V/b$ and a and b are constants (mV).

In this scheme, the depression of the maximum current may be accounted for by a voltage-independent blocking action of the ions, whereas the apparent shift in the activation range could be interpreted by the voltage-dependent blocking action. Calculated dissociation constants for Cd^{2+}, Ca^{2+} and Ba^{2+} are given in Table 2. Dissociation constants for voltage-dependent and voltage-independent components

of block appeared to vary independently, giving the variable voltage shifts and maximal current depressions shown in Fig. 9. These calculations provided a reasonable fit to the experimental data over wide ranges of block but there were some discrepancies in the predictions with very small and very large degrees of block (partly, perhaps, because of inherent errors of measurement at these extremes).

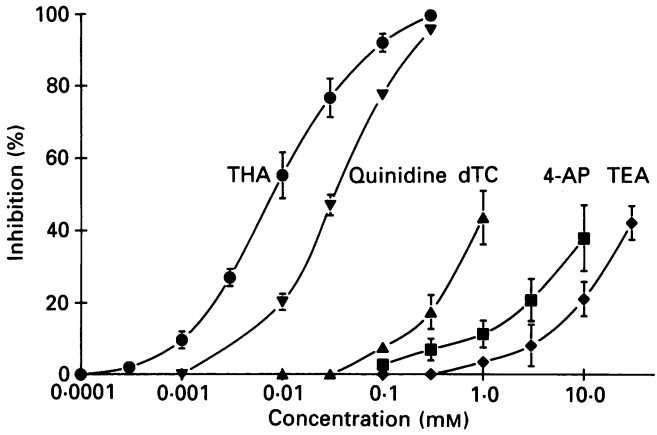

Fig. 10. Effects of some organic K^+ channel blocking drugs on $I_{K(M,ng)}$. Ordinate, percentage inhibition of $I_{K(M,ng)}$, measured from the amplitude of the deactivation relaxations observed during 1 s hyperpolarizing steps from −30 to −60 mV. Abscissa, concentration of blocking drug (mM, logarithmic scale). Points are means of five to seven experiments; bars = S.E.M. Drugs were: ●, 9-amino-1,2,3,4,-tetrahydroacridine (THA); ▼, quinidine; ▲, *d*-tubocurarine (dTC); ■, 4-aminopyridine (4-AP); ◆, tetraethylammonium (TEA).

Divalent cation block in sympathetic ganglia. In contrast to the above observations, divalent cation block of $I_{K(M)}$ in frog sympathetic ganglia appears not to be accompanied by a substantial shift in activation voltage (Adams *et al.* 1982*b*; Beech & Barnes, 1989; Tokimasa & Akasu, 1990). We tested this further in dissociated rat superior cervical sympathetic ganglion cells (see Marrion *et al.* 1989*b*). In agreement with previous observations on rat cells (Constanti & Brown, 1981), Ba^{2+} reduced the maximum amplitude of $I_{K(M)}$ by about 59% at 0·3 mM, 77% at 1 mM and 90% at 3 mM ($n = 3$). This effect was accompanied by a modest shift in half-activation voltage, of about 4·3 mV/e-fold concentration increase in $[Ba^{2+}]$. In contrast to NG108-15 cells, addition of Cd^{2+} (up to 1 mM), or increasing $[Ca^{2+}]$ from 0 to 10 mM (in the presence of 5 mM $[Mg^{2+}]$), did not reduce $I_{K(M)}$, but produced a similar shift in half-activation voltage to that produced by Ba^{2+} (about 4·3 mV/e-fold concentration increase). These shifts are much less than those observed in NG108-15 cells and may more easily be accounted for by a change in surface charge.

Organic potassium channel blockers

A number of organic K^+ channel blockers were tested for their effect on $I_{K(M,ng)}$. As shown in Fig. 10, $I_{K(M,ng)}$ was very insensitive to tetraethylammonium ($IC_{50} >$ 30 mM) or 4-aminopyridine ($IC_{50} > 10$ mM) and was less sensitive than the slow Ca^{2+}-activated K^+ current in these cells to *d*-tubocurarine (cf. Brown & Higashida, 1988*a*).

It was also insensitive to the peptide blocking agent apamin (up to 3 μM; $n = 3$), which blocks the slow Ca^{2+}-activated current in these cells (Hugues, Romey, Duval, Vincent & Lazdunski, 1982; Brown & Higashida, 1988*a*), or to dendrotoxin (up to 100 nM; $n = 2$). The most effective blocking agent tested was 9-amino-1,2,3,4-tetrahydroacridine (THA; IC_{50} about 8 μM); this IC_{50} is considerably less than the concentrations (0·5–1 mM) required to block $I_{K(M)}$ in rat sympathetic ganglia (Marsh, Hubbard & Brown, 1990). Quinine inhibited $I_{K(M,ng)}$ with an IC_{50} of about 30 μM.

Receptors coupled to $I_{K(M,ng)}$

Brown & Higashida (1988*b*) reported that bradykinin inhibited the M-like current recorded from microelectrode-impaled NG108-15 cells. We have recorded a comparable inhibition of $I_{K(M,ng)}$ in patch-clamped cells. Bath-perfused bradykinin (10 μM) inhibited $I_{K(M,ng)}$ by $34·5 \pm 2·6$% ($n = 13$) while pressure-applied bradykinin (100 μM; 13–55 kPa) inhibited $I_{K(M,ng)}$ by 65 ± 9% ($n = 8$). Compared with responses of microelectrode-impaled cells, patch-clamped cells appeared to be rather less sensitive to bradykinin and the response showed more severe desensitization. Thus, during bath application, $I_{K(M,ng)}$ recovered within 3–4 min, and no further effect could be obtained up to an hour later, while pressure application became ineffective after two or three tests.

A number of agonists at other potential transmitter receptors were also tested for their effect on $I_{K(M,ng)}$. Angiotensin II (1–10 μM) imitated the effect of bradykinin: a bradykinin-like action of angiotensin has previously been reported in these cells (Higashida, Wilson, Adler & Nirenberg, 1978) and in parent rat C6 glioma cells (Hopp, Reuter, Reiser & Hamprecht, 1987). No consistent or significant inhibition of $I_{K(M,ng)}$ was seen after applying the following other agonists ($n = 2$ or 3 in each case): acetylcholine (10 mM), muscarine (100 μM), methacholine (10 μM), noradrenaline (100 μM), adrenaline (100 μM), dopamine (100 μM), histamine (100 μM), enkephalin (1 μM), glycine (100 μM), γ-aminobutyric acid (100 μM), baclofen (500 μM), 5-hydroxytryptamine (0·1–10 μM). (The latter produced a large, rapidly desensitizing inward current, as previously reported in these cells (Yakel & Jackson, 1988) but did not clearly inhibit $I_{K(M,ng)}$.)

Functions of $I_{K(M,ng)}$

Three physiological functions of $I_{K(M)}$ in sympathetic neurones have been suggested previously (see Brown, 1988). Firstly, it may contribute to the resting potential recorded in microelectrode-impaled cells (Adams *et al.* 1982*a*), although probably not in unimpaled (Tosaka, Tasaka, Miyazaki & Libet, 1983) or in patch-clamped (Jones, 1989) cells. Second, it confers strong outward rectification to the steady-state current–voltage curve, and thereby reduces membrane potential responses to depolarizing currents. Thirdly, it can induce accommodation of action potential trains.

To find out whether $I_{K(M,ng)}$ might have comparable effects in NG108–15 cells, we tested the effects of inhibiting $I_{K(M,ng)}$ on steady-state current–voltage curves, resting potential and action potential responses to current injection. Since bradykinin produced only partial inhibition, and desensitized strongly, we used Ba^{2+} to inhibit $I_{K(M,ng)}$.

Current–voltage curves

Figure 11 shows the effect of Ba^{2+} on the steady-state current–voltage (I–V) curve determined using voltage ramps. In normal (3 mM) [K^+] solution, the I–V curve shows strong outward rectification positive to −60 mV, as $I_{K(M,ng)}$ is activated.

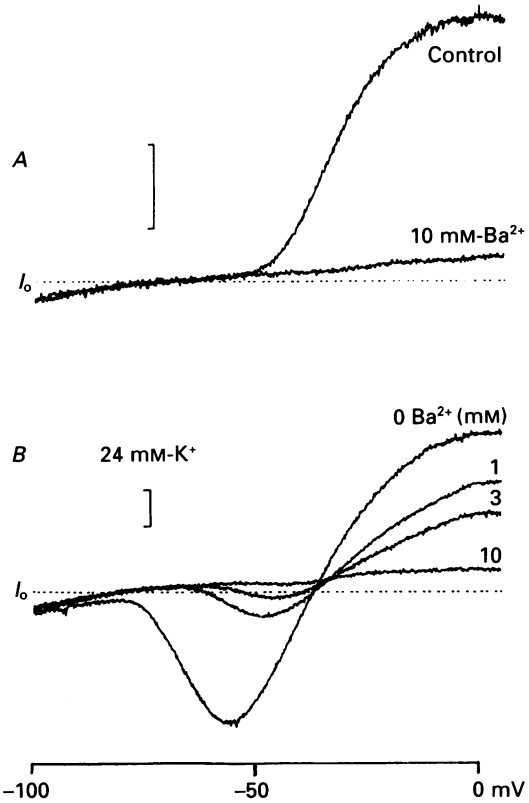

Fig. 11. Effects of external Ba^{2+} ions on steady-state current–voltage curves, determined using voltage ramps from 0 mV (holding potential) to −100 mV. Interrupted lines show zero-current level (I_0). *A*, effect of 10 mM-Ba^{2+} recorded in normal (3 mM $[K^+]_o$) solution. *B*, effect of increasing concentrations of Ba^{2+} (0, 1, 3 and 10 mM) on the ramp current–voltage curves recorded in 24 mM $[K^+]_o$. *A* and *B* are from the separate cells. Note that Ba^{2+} reduced or abolished the rectification positive to −80 mV associated with the activation of $I_{K(M,ng)}$ but did not affect currents negative to −80 mV. Calibration bars 0·5 nA.

Thus, in the example illustrated in Fig. 11*A*, slope conductance increased from $< 1{\cdot}8$ nS at −70 mV to about 40 nS at −30 mV. In six such tests on different cells with resting conductances at −70 mV of between 1 and 3 nS, the mean slope conductance (±S.E.M.) at −30 mV was 60±5·4 nS. (This may overestimate the maximum slope conductance induced by $I_{K(M,ng)}$ itself, because of a countervailing, time-independent inward current at potentials positive to −20 mV. Notwith-

standing, the conductance in the range where $I_{K(M,ng)}$ is activated is clearly many times larger than the leak conductance.) Ba^{2+} (10 mM) eliminated this outward rectification without affecting the I–V curve at negative potentials.

Since $I_{K(M,ng)}$ deactivates at potentials positive to E_K in 3 mM $[K^+]$, and hence is always outward, it seemed useful to test Ba^{2+} under conditions where $I_{K(M,ng)}$ was inward. Hence, we repeated these experiments in 24 mM $[K^+]$ (Fig. 11*B*): E_K was then about −36 mV (which was also the resting potential), and $I_{K(M,ng)}$ appears as an inward current negative to E_K and an outward current positive to E_K. Ba^{2+} reduced both inward and outward rectification. In fact, Ba^{2+} reduced the inward component more than the outward component, but this is a consequence of the positive shift of the activation curve (see Fig. 9), as confirmed by the shift in activation threshold for the inward current in Fig. 11*B*.

Thus, so far as steady-state currents are concerned, Ba^{2+} blocked all rectification associated with activation of $I_{K(M,ng)}$, without affecting membrane current below the threshold for $I_{K(M,ng)}$ activation.

Resting potential

In 3 mM $[K^+]_o$, the ramp I–V curves crossed the zero-current line at potentials just negative to the threshold for outward rectification, and addition of Ba^{2+} had no significant effect on this zero-current potential. This implies that $I_{K(M,ng)}$ may not be activated at resting potential. However, since the ramps were driven from 0 mV, other currents which might have been present normally at rest might have been inactivated. Hence, we tested the effect of adding 10 mM-Ba^{2+} in a series of cells patched at their resting potential with electrodes containing 3 mM-EGTA and sufficient Ca^{2+} to set free $[Ca^{2+}]$ to about 40 nM. The mean resting potential (±S.E.M.) was $-69{\cdot}4 \pm 4{\cdot}5$ mV ($n = 7$). Ba^{2+} did not change the resting potential in any of the seven cells tested. This confirms that $I_{K(M,ng)}$ did not contribute directly to resting membrane current under our recording conditions, in agreement with the conclusions of Jones (1989) in frog ganglion cells recorded under similar conditions. (It should be noted that the resting potential of these cells was considerably more negative than that of the microelectrode-impaled cells studied previously (Brown & Higashida, 1988*a* and *b*), which were depolarized by Ba^{2+} or bradykinin.)

Excitability

Depolarization of differentiated NG108-15 cells induces Na^+-dependent action potentials (see e.g. Hamprecht, 1977). Our sample of cells normally showed strong accommodation of action potential discharges (Fig. 12*A*). In the presence of Ba^{2+} ions, this accommodative property was reduced, such that the cells became capable of sustained trains of action potentials at frequencies of up to 9 Hz or so (Fig. 12*B*). This resembles the behaviour of sympathetic neurones in the presence of Ba^{2+} or of the M-current inhibitor, muscarine (see Fig. 10 in Brown, 1988). Although NG108-15 cells possess other K^+ currents than $I_{K(M,ng)}$ which might also be inhibited by Ba^{2+} ions, this appeared not to be the prime cause of the increased action potential train length. Thus, tetraethylammonium or 4-aminopyridine, which respectively inhibit the fast Ca^{2+}-activated K^+-current (Brown & Higashida, 1988*a*) and delayed rectifier current (Robbins & Sim, 1990), prolonged the duration of single action

potentials but did not induce repetitive discharges. Also, the effect of Ba^{2+} was not replicated by *d*-tubocurarine or apamin (Fig. 12), which block the slow Ca^{2+}-activated K^+ current (Hugues *et al.* 1982; Brown & Higashida, 1988*a*). (The latter current was, in any case, much less prominent in these patch-clamped cells than in the microelectrode-impaled cells described by Brown & Higashida, 1988*a*).

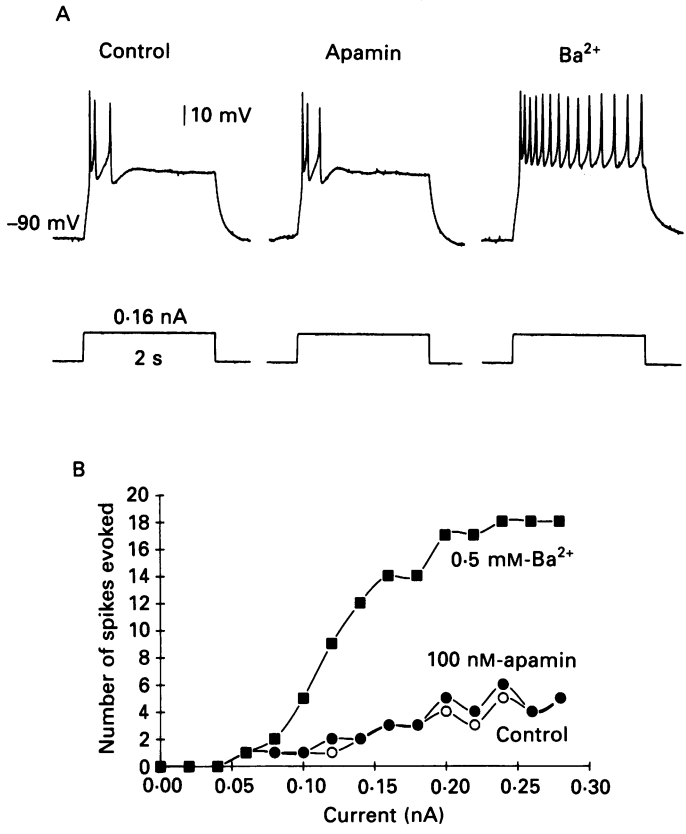

Fig. 12. Effects of apamin and Ba^{2+} on action potential discharges in an NG108-15 cell. Records in *A* show action potentials induced by 2 s, +0·16 nA depolarizing currents injected at a holding potential of −90 mV in the absence of drug (control) and then in the presence of 100 nM-apamin or 0·5 mM-Ba^{2+}. *B* shows the relation between the number of action potentials generated during 2 s depolarization (ordinate) and the magnitude of the depolarizing current (abscissa). Note that Ba^{2+}, but not apamin, facilitates repetitive action potential discharge.

DISCUSSION

The K^+ current studied in these experiments clearly accords with that previously identified in microelectrode-impaled cells as an M-current (Brown & Higashida, 1988*a*). Thus, it seems to be well preserved without appreciable 'run-down' in cells internally dialysed with a patch electrode, even without ATP or GTP in the pipette solution: and in fact addition of ATP and GTP made no obvious difference to the magnitude or longevity of the current. The main difference in whole-cell clamp was

the somewhat weaker inhibition, and more profound desensitization, following application of bradykinin. We do not yet know the reason for this, but would note that this also does not seem to be dependent on the presence or absence of ATP and GTP.

The principal question we have addressed is how far the current in NG108-15 cells (which, for the purposes of the present paper, we have provisionally designated as

TABLE 3. Kinetics of M-currents and M-like currents in different neural cells

Cell type...	Frog sympathetic	Frog sympathetic	Rat sympathetic	Salamander rod photoreceptor	NG108-15 hybrid
Current	$I_{K(M)}$	$I_{K(M)}$	$I_{K(M)}$	I_{Kx}	$I_{K(M,ng)}$
Recording*	m/e (2)	p/e	m/e (1)	p/e	p/e
Temperature	20 °C	22 °C	22 °C	22 °C	35 °C
V_0 (mV)	−35	−52	−45	−46	−44
a (mV)	10	7	8·7	4·6	8·1
$\tau(V_0)$ (ms)	150	—	100	280	230
Reference	1	2	3	4	5

References: (1) Adams *et al.* (1982*a*) (*R. catesbiana*); (2) Selyanko *et al.* (1990) (*R. pipiens*); (3) Constanti & Brown (1981); (4) Beech & Barnes (1989); (5) present paper.

* m/e (2) = twin-microelectrode voltage clamp; m/e (1) = single-microelectrode voltage clamp; p/e = patch electrode (whole-cell configuration).

$I_{K(M,ng)}$) resembles or differs from $I_{K(M)}$ in sympathetic neurones, or from M-like currents seen in other cells; and thus how far NG108-15 cells serve as reasonable models for studies on M-currents in general. Our observations show that $I_{K(M,ng)}$ *resembles* the ganglionic M-current in (i) macroscopic current kinetics, (ii) functional effects, and (ii) sensitivity to internal Ca^{2+}, but *differs* in several pharmacological respects. These features are discussed in turn below.

Kinetics

These clearly resemble those of the M-current originally described in bullfrog sympathetic neurones (Adams *et al.* 1982*a*). Thus, unlike the conventional delayed rectifier current, activation of $I_{K(M,ng)}$ follows a simple exponential time course, with no obvious co-operativity. Further, both steady-state activation curves and deactivation time constants appear to follow a simple Boltzmann distribution as though governed by a single gating 'particle' with an effective valency of about +3. The activation threshold and half-activation voltage are slightly more negative than those originally reported for bullfrog sympathetic neurones (Adams *et al.* 1982*a*), but are close to those reported in rat sympathetic neurones (Constanti & Brown, 1981), or in amphibian neurones when recorded with patch electrodes (Selyanko, Smith & Zidichouski, 1990) (see Table 3).

Function

Functionally, also, $I_{K(M,ng)}$ behaves like $I_{K(M)}$. Thus, it appears to contribute to the control of repetitive firing behaviour (see Fig. 12) in the manner originally proposed for sympathetic neurones (Adams *et al.* 1982*b*; Brown, 1983). However, while it may

assist the cells in resisting perturbations of resting potential induced by depolarizing currents or by microelectrode damage (cf. Adams *et al.* 1982*a*), $I_{K(M,ng)}$ does not appear to contribute directly to the resting potential in the majority of cells, in agreement with recent conclusions in frog ganglion cells (Jones, 1989).

Internal Ca^{2+}

There have been several reports that $I_{K(M)}$ in frog sympathetic ganglia is inhibited by transient increases in intracellular [Ca^{2+}] (Tokimasa, 1985; Pfaffinger *et al.* 1988; Akaike & Sadoshima, 1989; Marrion *et al.* 1989*a*; Marrion *et al.* 1991). We have obtained evidence for the same effect in NG108-15 cells following an influx of Ca^{2+} through voltage-gated Ca^{2+} channels or the release of Ca^{2+} from internal stores by caffeine. On the other hand (but also in agreement with observations on ganglion cells: Pfaffinger *et al.* 1988; Beech, Bernheim, Mathie & Hille, 1991) there was no obvious change in the amplitude of $I_{K(M,ng)}$ when cells were patched with electrodes containing different amounts of free [Ca^{2+}], or even in the same cells when patched with two different electrodes containing low and high [Ca^{2+}]. One explanation for this might be that, while $I_{K(M,ng)}$ might be affected by sudden changes in internal [Ca^{2+}], some form of adaptation occurs during sustained or gradual changes. Marrion *et al.* (1991) observed reasonably sustained (2 min) changes in $I_{K(M)}$ in bullfrog sympathetic neurones after raising $[Ca^{2+}]_i$ by flash photolysis of Nitr-5, but full equilibration of BAPTA or EGTA between the pipette solution and the cytoplasm of these large NG108-15 cells is probably slower than this (see Beech *et al.* 1991). Thus, while substantial filling with Indo-1 had occurred by 5 min, a slow increase in fluorescence intensity up to 15 min after patching was common. For this reason, we allowed 15 min between measurements of $I_{K(M,ng)}$ when re-patching with different electrodes: this may be sufficient time for substantial adaptation. (Although caffeine produced a sustained inhibition of $I_{K(M,ng)}$ for up to 15 min, intracellular [Ca^{2+}] was not constant during this time in the presence of caffeine, but showed one or more 'spikes' of high [Ca^{2+}], as previously noted in frog ganglion cells (Pfaffinger *et al.* 1988; Marrion *et al.* 1989*a*): hence, caffeine is not the best tool for producing controlled, steady increases in intracellular [Ca^{2+}].)

Pharmacology

$I_{K(M,ng)}$ showed three pharmacological differences from most reported sympathetic neurone M-currents. First, $I_{K(M,ng)}$ is more sensitive than $I_{K(M)}$ to some organic blockers, most notably 9-aminotetrahydroacridine (cf. Marsh *et al.* 1990). Secondly, it is highly sensitive to block by certain divalent cations (but see Tokimasa & Akasu, 1990). Thirdly, $I_{K(M,ng)}$ is not significantly inhibited by acetylcholine or muscarine under our patch-clamp recording conditions.

The latter is somewhat embarrassing for a current putatively designated an 'M-current'. However, the explanation is simple (though interesting): the muscarinic receptor in NG108-15 cells is the wrong type of receptor. Thus, the endogenous receptor is the m4-genotype (Peralta, Ashkenazi, Winslow, Smith, Ramachandran & Capon, 1987; Fukuda *et al.* 1988), which does not seem to couple efficiently to $I_{K(M,ng)}$; in contrast, $I_{K(M,ng)}$ can be readily inhibited by acetylcholine or muscarine

in NG108-15 cells transformed to express either m1- or m3-receptors (Fukuda *et al.* 1988; Neher *et al.* 1988; Robbins *et al.* 1991). This agrees with deductions from pharmacological tests on rat ganglion cells, where the corresponding M_1-phenotype seems to be responsible for M-current inhibition (Marrion *et al.* 1989). The same explanation probably accounts for the resistance of PC12 phaeochromocytoma M-like currents to muscarine (Villaroel, Marrion, Lopez & Adams, 1989), since these also appear to express m4-receptors (Michel, Stefanich & Whiting, 1989). It might equally well apply to the muscarine resistance of the M-current in C-cells of bullfrog sympathetic ganglia (Jones, 1987), and of the kinetically similar current I_{Kx} in salamander rods (Beech & Barnes, 1989), though the endogenous receptor present in these cells (if any) is unknown. The key feature required for M-current inhibition seems to be that the receptor concerned should be able to stimulate phosphatidylinositide breakdown (see Fukuda *et al.* 1988), and possibly to raise intracellular [Ca^{2+}] (Neher *et al.* 1988; Kirkwood, Simmons, Mather & Lisman, 1991; but see Beech *et al.* 1991). Thus, because of this subtype dependence, absence of inhibition by muscarine does not, of itself, suffice to disqualify $I_{K(M,ng)}$ (or possibly I_{Kx}) as an M-current.

The sensitivity of $I_{K(M,ng)}$ to external divalent cations is more problematical. Since there was quite a good correlation between the concentrations of different divalent cations required to inhibit $I_{K(M,ng)}$ and those needed to inhibit I_{Ca}, one obvious possibility is that $I_{K(M,ng)}$ is a species of Ca^{2+}-activated K^+ current, requiring a priming influx of Ca^{2+} through voltage-gated Ca^{2+} channels for its activation (as earlier suggested for $I_{K(M)}$ in frog ganglion cells: Koketsu *et al.* 1982). However, several observations argue strongly against this possibility. First, several other Ca^{2+} channel blocking agents (La^{3+}, nifedipidine, ω-conotoxin) failed to block $I_{K(M,ng)}$ in concentrations which blocked I_{Ca}. Second, Cd^{2+} still blocked $I_{K(M,ng)}$ in the absence of external Ca^{2+}. Third, omission of external Ca^{2+} *increased* $I_{K(M,ng)}$, instead of reducing it, whereas the slow Ca^{2+}-activated after-current is abolished by this procedure (Brown & Higashida, 1988*a*). Taken in conjunction with the fact that raising intracellular Ca^{2+} inhibits $I_{K(M,ng)}$ (see above), these observations suggest that the effect of the divalent cations is not secondary to a reduction in Ca^{2+} entry but instead results from a direct blocking action of the ions on the K^+ channels from the outside. This extends to divalent cations which not only block Ca^{2+} channels but which (like Ba^{2+}, Sr^{2+} and Ca^{2+} itself) act as charge carriers for the Ca^{2+} channel.

This blocking action seems complex, in that both voltage sensitivity and maximum conductance are affected. Since these two parameters are affected differentially by Ca^{2+}, Ba^{2+} and Cd^{2+}, it is difficult to encompass the data within a frame work involving a single binding site. We have interpreted the data in terms of two binding sites: one which is sensitive to membrane field and hence confers voltage dependence on the binding constant, and one which is insensitive to voltage. However, this is not entirely satisfactory since, even with two binding constants, the experimental data deviate from predictions at low and high block extremes. Further, the voltage sensitivities of the voltage-dependent binding constants vary for the different cations, for 14·7 mV for Ba^{2+} to 5·8 mV for Cd^{2+}. Since this is inversely proportional to their hydrated ionic radii (Table 2), perhaps Ba^{2+} penetrates deeper within the channel than Ca^{2+} or Cd^{2+}. An alternative possibility is that these cations

modify the voltage gating of $I_{K(M,ng)}$, as suggested by Beech & Barnes (1989) for Ba^{2+} blocks of I_{Kx}. If so, this cannot be through a simple surface charge screening or binding effect because of the variable shifts in half-activation voltage; nor can this effect alone readily account for the reduced maximum conductance.

These pharmacological peculiarities of $I_{K(M,ng)}$, combined with conventional M-type kinetic behaviour, suggest that there might be a family of M-type K^+ channels akin to the family of delayed rectifier channels, which might also include the salamander rod current I_{Kx}. Notwithstanding, since $I_{K(M,ng)}$ shows similar kinetics and comparable responses to internal Ca^{2+}, and to agonists for PLC-linked receptors, to those of ganglionic M-currents, NG108-15 cells seem quite reasonable cells for further work on M-currents in general.

This work was supported by grants from the Medical Research Council. We thank Yvonne Vallis for help with tissue culture.

REFERENCES

ADAMS, P. R., BROWN, D. A. & CONSTANTI, A. (1982*a*). M-currents and other potassium currents in bullfrog sympathetic neurones. *Journal of Physiology* **330**, 537–562.

ADAMS, P. R., BROWN, D. A. & CONSTANTI, A. (1982*b*). Pharmacological inhibition of the M-current. *Journal of Physiology* **332**, 223–262.

AKAIKE, N. & SADOSHIMA, J. (1989). Caffeine affects four different ionic currents in the bull-frog sympathetic neurones. *Journal of Physiology* **412**, 221–244.

BEECH, D. J. & BARNES, S. (1989). Characterization of a voltage-gated K^+ channel that accelerates the rod response to dim light. *Neuron* **3**, 573–581.

BEECH, D. J., BERNHEIM, L., MATHIE, A. & HILLE, B. (1991). Intracellular Ca^{2+} buffers disrupt muscarinic suppression of Ca^{2+} current and M-current in rat sympathetic neurons. *Proceedings of the National Academy of Sciences of the USA* **88**, 652–656.

BROWN, D. A. (1983). Slow cholinergic excitation – a mechanism for increasing neuronal excitability. *Trends in Neurosciences* **6**, 302–307.

BROWN, D. A.(1988). M-currents. In *Ion Channels*, vol. 1, ed. NARAHASHI, T., pp. 55–94. Plenum Publishing Corporation, New York.

BROWN, D. A. & ADAMS, P. R. (1980). Muscarinic suppression of a novel voltage-sensitive K^+-current in a vertebrate neurone. *Nature* **283**, 673–676.

BROWN, D. A. & HIGASHIDA, H. (1988*a*). Voltage- and calcium-activated potassium currents in mouse neuroblastoma × rat glioma hybrid cells. *Journal of Physiology* **397**, 149–165.

BROWN, D. A. & HIGASHIDA, H. (1988*b*). Membrane current responses of NG108-15 mouse neuroblastoma × rat glioma hybrid cells to bradykinin. *Journal of Physiology* **397**, 167–184.

BROWN, D. A. & ROBBINS, J. (1990). Divalent and trivalent cations inhibit a voltage-dependent potassium current in rodent neuroblastoma × glioma hybrid (NG108-15) cells. *Journal of Physiology* **424**, 24*P*.

CLOUES, R. & ROBBINS, J. (1991). Dependence of the inositol trisphosphate evoked potassium current on anions in whole-cell recordings from rodent neuroblastoma × glioma hybrid cells. *Journal of Physiology* **438**, 222*P* .

CONSTANTI, A. & BROWN, D. A. (1981). M-currents in voltage-clamped mammalian sympathetic neurones. *Neuroscience Letters* **24**, 289–294.

DOCHERTY, R. J. (1988). Gadolinium selectively blocks a component of calcium current in rodent neuroblastoma × glioma hybrid (NG108-15) cells. *Journal of Physiology* **398**, 33–47.

FINKEL, A. S. & REDMAN, S. (1984). Theory and operation of a single microelectrode voltage clamp. *Journal of Neuroscience Methods* **11**, 101–127.

FUKUDA, K., HIGASHIDA, H., KUBO, T., MAEDA, A., AKIBA, I., BUJO, H., MISHINA, M. & NUMA, S. (1988). Selective coupling with K^+ currents of muscarinic acetylcholine receptor subtypes in NG108-15 cells. *Nature* **335**, 355–358.

GRUNER, W., MARRION, N. V. & ADAMS, P. R. (1989). Three kinetic components to M-currents in bullfrog sympathetic neurons. *Society for Neuroscience Abstracts* **15**, 990.

GRYNKIEWICZ, G., POENIE, M. & TSIEN, R. Y. (1985). A new generation of Ca^{2+} indicators with greatly improved fluorescence properties. *Journal of Biological Chemistry* **260**, 3440–3450.

HAGIWARA, S. & BYERLY, L. (1981). Calcium channel. *Annual Review of Neuroscience* **4**, 69–125.

HAMPRECHT, B. (1977). Structural, electrophysiological and pharmacological properties of neuroblastoma–glioma cell hybrids in cell culture. *International Review of Cytology* **49**, 99–170.

HIGASHIDA, H., WILSON, S. P., ADLER, M. & NIRENBERG, M. (1978). Synapse formation by neuroblastoma hybrid cell lines. *Society for Neuroscience Abstracts* **4**, 591.

HOPP, R.-P., REUTER, G., REISER, G. & HAMPRECHT, B. (1987). Angiotensin evokes in polyploid rat glioma cells hyperpolarization–depolarization responses and cross-desensitizes with bradykinin. *Brain Research* **412**, 175–178.

HUGUES, M., ROMEY, G., DUVAL, D., VINCENT, J. P. & LAZDUNSKI, M. (1982). Apamin as a selective blocker of the calcium-dependent potassium channel in neuroblastoma cells: voltage-clamp and biochemical characterization of the toxin receptor. *Proceedings of the National Academy of Sciences of the USA* **79**, 1308–1312.

JONES, S. W. (1987). A muscarine-resistant M-current in C cells of bullfrog sympathetic ganglia. *Neuroscience Letters* **74**, 309–314.

JONES, S. W. (1989). On the resting potential of isolated frog sympathetic neurones. *Neuron* **3**, 153–161.

KELLY, M. E. M. & PENNEFATHER, P. (1989). The kinetics of M-currents (I_M) recorded in bullfrog sympathetic ganglion cells. *Society for Neuroscience Abstracts* **15**, 1145.

KIRKWOOD, A., SIMMONS, M. A., MATHER, R. J. & LISMAN, J. E. (1991). Muscarinic suppression of the M-current is mediated by a rise in internal Ca^{2+} concentration. *Neuron* **6**, 1009–1014.

KOKETSU, K., AKASU, T. & MIYAGAWA, M. (1982). Identification of g_K systems activated by $[Ca^{2+}]_{in}$. *Brian Research* **243**, 369–372.

KUBA, K. (1980). Release of calcium ions linked to the activation of potassium conductance in a caffeine treated sympathetic neurone. *Journal of Physiology* **298**, 251–269.

MCFADZEAN, I., MULLANEY, I., BROWN, D. A. & MILLIGAN, G. (1989). Antibodies to the GTP-binding proteins, G_o, antagonize noradrenaline-induced calcium current inhibition in NG108-15 hybrid cells. *Neuron* **3**, 177–182.

MCLAUGHLIN, S. G. A., SZABO, G. & EISENMAN, G. (1971). Divalent cations and the surface potential of charged phospholipid membrane. *Journal of General Physiology* **58**, 667–687.

MARRION, N. V., MARSH, S. J., BURBACH, B. J., BROWN, D. A. & ADAMS, P. R. (1989*a*). Effect of ruthenium red and ryanodine on the caffeine-induced rise of intracellular calcium in vertebrate sympathetic neurons. *Society for Neuroscience Abstracts* **15**, 16.

MARRION, N. V., SMART, T. G., MARSH, S. J. & BROWN, D. A. (1989*b*). Muscarinic suppression of the M-current in the rat sympathetic ganglion is mediated by receptors of the M_1-subtype. *British Journal of Pharmacology* **98**, 557–573.

MARRION, N. V., ZUCKER, R. S., MARSH, S. J. & ADAMS, P. R. (1991). Modulation of M-current by intracellular Ca^{2+}. *Neuron* **6**, 533–545.

MARSH, S. J., HUBBARD, A. & BROWN, D. A. (1990). Some actions of 9-amino-1,2,3,4-tetrahydroacridine (THA) on cholinergic transmission and membrane currents in rat sympathetic ganglia. *European Journal of Neuroscience* **2**, 1127–1134.

MICHEL, A. D., STEFANICH, E. & WHITING, R. L. (1989). PC12 phaeochromocytoma cells contain an atypical muscarinic receptor binding site. *British Journal of Pharmacology* **97**, 914–920.

NEHER, E., MARTY, A., FUKUDA, K., KUBO, T. & NUMA, S. (1988). Intracellular calcium release mediated by two muscarinic receptor subtypes. *FEBS Letters* **240**, 88–94.

OHMORI, H. & YOSHII, M. (1979). Surface potential reflected in both gating and permeation mechanisms of sodium and calcium channels of tunicate egg cell membrane. *Journal of Physiology* **267**, 429–463.

PERALTA, E. G., ASHKENAZI, A., WINSLOW, J. W., SMITH, D. H., RAMACHANDRAN, J. & CAPON, D. J. (1987). Distinct primary structures, ligand-binding properties and tissue-specific expression of four human muscarinic acetylcholine receptors. *EMBO Journal* **6**, 3923–3939.

PFAFFINGER, P. J., LEIBOWITZ, M. D., SUBERS, E. M., NATHANSON, W., ALMERS, W. & HILLE, B. (1988). Agonists that suppress M-current elicit phosphoinositide turnover and Ca^{2+} transients, but these events do not explain M-current suppression. *Neuron* **1**, 477–484.

POPOV, E. G., GAVRIOLY, I. Y., POZIN, E. Y. & GABBASOV, Z. A. (1988). Multiwavelength method for measuring concentration of free calcium using the fluorescent probe Indo-1. *Archives of Biochemistry and Biophysics* **261**, 91–96.

ROBBINS, J., CAULFIELD, M. P., HIGASHIDA, H. & BROWN, D. A. (1991). Genotypic M3-muscarinic receptors preferentially inhibit M-currents in DNA-transfected NG108-15 neuroblastoma-× glioma hybrid cells. *European Journal of Neuroscience* **3**, 820–824.

ROBBINS, J. & SIM, J. A. (1990). A transient outward current in NG108-15 neuroblastoma × glioma hybrid cells. *Pflügers Archiv* **416**, 130–137.

SALA, F. & HERNANDEZ-CRUZ, A. (1990). Calcium diffusion modelling in a spherical neuron. Relevance of buffering properties. *Biophysical Journal* **57**, 313–324.

SELYANKO, A. A., SMITH, P. A. & ZIDICHOUSKI, J. A. (1990). Effects of muscarine and adrenaline on neurones from *Rana pipiens* sympathetic ganglia. *Journal of Physiology* **425**, 471–500.

SHANNON, R. D. (1976). Revised effective ionic radii and systematic studies of interaction distances in halides and chalcogenides. *Acta Crystallographia* **A32**, 751–767.

TOKIMASA, T. (1985). Intracellular Ca^{2+} ions inactivate K^+-current in bullfrog sympathetic neurons. *Brain Research* **387**, 386–391.

TOKIMASA, T. & AKASU, T. (1990). Extracellular calcium ions are required for muscarine-sensitive potassium current in bullfrog sympathetic neurons. *Journal of the Autonomic Nervous System* **29**, 163–174.

TOSAKA, T., TASAKA, I., MIYAZAKI, T. & LIBET, B. (1983). Hyperpolarization following activation of K^+ channels by excitatory postsynaptic potentials. *Nature* **305**, 148–150.

VILLAROEL, A., MARRION, N. V., LOPEZ, H. & ADAMS, P. R. (1989). Bradykinin inhibits a potassium M-like current in rat phaeochromocytoma PC12 cells. *FEBS Letters* **255**, 42–46.

WAHL, M., LUCHERINI, M. J. & GRUENSTEIN, E. (1990). Intracellular Ca^{2+} measurements with Indo-1 in substrate-attached cells: advantages and special considerations. *Cell Calcium* **11**, 487–500.

WOODHULL, A. M. (1973). Ionic blockage of sodium channels in nerve. *Journal of General Physiology* **61**, 687–708.

YAKEL, J. L. & JACKSON, M. B. (1988). 5-HT_3 receptors mediate rapid responses in cultured hippocampus and a clonal cell line. *Neuron* **1**, 615–621.